A KINEMATIC MODEL FOR HYSTERETIC DISSIPATION OF VIBRATION ENERGY FOR TORSIONAL DAMPER AND DETUNER (TDD)

Alexander N. DANILIN
Moscow Aviation Institute – Volokolamskoye sh., 4, A-80 GSP 3, 125993, Moscow, Russia
andanilin@yandex.ru
Alexander A. VINOGRADOV
JSC "Elektrosetstroyproject" – Vysokovoltny pr., 1, str. 36, 127566, Moscow, Russia
alex.vin@essp.ru
Jean-Louis LILIEN
University of Liege, Institute Montefiore Sart Tilman B28, 4000, Liege, Belgium
lilien@montefiore.ulg.ac.be

Introduction

Torsional Damper and Detuner (TDD) is a mechanism for detuning and attenuation of low-frequency oscillations of OHL conductors galloping [1,2]. The oscillation energy is dissipated in the damping unit (DU), which represents a structure of two disks interconnected by the joint revolution axis and an ensemble of viscous-elastic elements, which react in relative rotation of disks. One of the disks is a leader and is connected to the phase conductors via a rigid frame. Another disk is a follower and is connected to the balancing lever of pendulum type.

A mathematic model of the TDD functionality has been developed for selection of geometric, mass and viscous-elastic parameters enabling the effective operation of the device in the frequency range 0.2-0.6 Hz [3]. This model takes into account the hysteretic type of power dissipation appropriate to the type of DU under consideration.

The process of hysteretic deformation of viscous-elastic elements due to their displacement inside DU is of high complexity and it cannot be subject of a rigorous mathematic description. That is why the approximate methods are traditionally employed making use of experimental data. One of the approaches consists in substitution of hysteresis by viscous-elastic deformation using the tension-compression diagrams of the elastoplastic samples and a logarithmic decrement of vibrations. Another possible approach consists in the assignment of the deformation diagram in accordance to model of Drucker-Prager. According to this model, the hysteresis diagram is represented by a parallelogram inclined by a certain angle to the coordinate axes. However, the use of such models may cause serious errors in selection of TDD structural parameters, since they do not take into account the shape and size of minor loops on the deformation diagram. Representation of the DU stiff and dissipation parameters turns out unstable and, occasionally, incorrect.

In this work, a kinematic model of hysteresis process is suggested which relates upon the hysteresis diagrams really obtained in tests. According to it, the torque moment and corresponding angle of torsion are related one to another via a special differential equation of the first order, its coefficients being defined from experimental values. Due to this, one succeeds to describe, in a single equation, an infinite set of similar cycles; each of them is uniquely defined by a position of a starting point on a deformation diagram inside a limit cycle. Similarity of these curves is defined by their asymptotic approximation to the limit cycle curve.

1. The TDD's mechanical model

A simplified TDD's mechanical model can be considered as a system (see Fig. 1) of driving (1) and driven (2) disks, a balancer or lever (3), rubber balls (4) and, in a more general sense, an elastic insert (5) that connects a driven disk and a balancer.

Let φ_1, φ_2, φ_3 are rotation angles of driving and driven disks and balancer respectively that are counted from vertical and positive if turning is performed anticlockwise. Moments, arising as a result of TDD deformation and acting on disks and a balancer, are shown in Fig. 2.

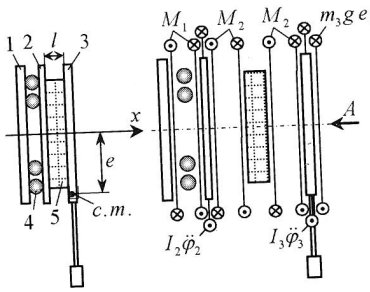

Fig. 1. Drawing of elementary TDD

Fig. 2. Moments of interaction of TDD components

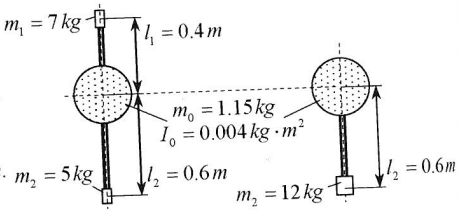

a) Inertia balancer b) Gravitational balancer

Fig. 3. Different variants of TDD balancer

In this picture M_1 is a moment generated by interaction of driving and driven disks via the system of rubber balls; M_2 is a moment producing torsion of an elastic insert; $m_3 g\, e \sin\varphi_3$ is a moment generated by balancer gravity force $m_3 g$ due to central mass eccentricity e (*c.m.*); $I_2\ddot{\varphi}_2$ is a inertia moment of a driven disk, where I_3 – polar moment of inertia of a balancer relative to x axis.
For the driven disk and the balancer we have the following equations of equilibrium

$$\begin{aligned} I_2\ddot{\varphi}_2 + M_1 - M_2 &= 0, \\ I_3\ddot{\varphi}_3 + M_2 + m_3 g\, e \sin\varphi_3 &= 0. \end{aligned} \tag{1}$$

The moment $M_1(\varphi_2 - \varphi_1)$ is formed by moments of interaction of driving and driven disks by several rows of rubber balls running in their troughs or spout guides. It is assumed that the moment M_2 is proportional to the twist angle $\varphi_3 - \varphi_2$ of the elastic insert. Then, according to the Hook's law, $M_2 = (\varphi_3 - \varphi_2)(GJ_t/l)$, where GJ_t is torsion stiffness of an elastic insert.
The law of motion of the driving disk is assumed to be a form: $\varphi_1(t) = \Phi \sin\omega t$, where Φ and ω are amplitude and frequency of harmonic motion.
Thus, the system of equations (1), describing periodic TDD motion under harmonic disturbance taking into account initial conditions, can be written in a form

$$I_2\ddot{\varphi}_2 = (\varphi_3 - \varphi_2)\frac{GJ_t}{l} - M_1(\varphi_2 - \varphi_1), \quad I_3\ddot{\varphi}_3 = -(\varphi_3 - \varphi_2)\frac{GJ_t}{l} - m_3 g\, e \sin\varphi_3; \tag{2}$$
$$\varphi_1 = \Phi \sin\omega t; \quad \varphi_2(0) = \dot{\varphi}_2(0) = \varphi_3(0) = \dot{\varphi}_3(0).$$

Possible variants of a balancer that has been used for calculations are given in Fig. 3.

2. Kinematic model for hysteretic dissipation of vibration energy

Let's turn to hysteresis diagrams $M = M(\alpha)$ obtained by series of experiments on the basis of the TDD test rig (at ESSP). Some of them are shown in Fig. 4.
It is obvious that if we start from a point inside region, bounded by the limit cycle curves, our curve will tend to a limit cycle curve asymptotically. It is true for both "loading" and "unloading" processes:

these are the same and the difference between them consists in the direction of angular displacement (and the moment applied). Thus, the given limit cycle curve determines the class of similar curves that have the unique asymptotical curve. The common asymptotic is a definition of similarity for internal curves actually (separately for "loading" and "unloading" cases). This fact allows developing analogy with behavior of the asymptotic solutions of differential equations. These solutions are determined identically by the integration constants but tend to a common asymptotic curve.

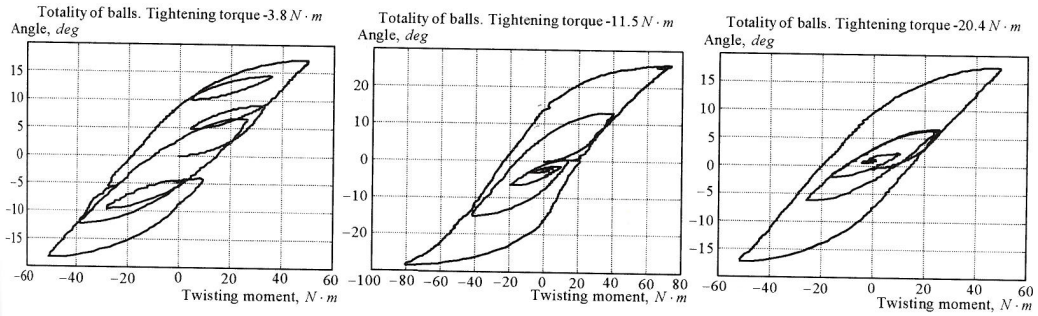

Fig. 4. Examples of complete and local hysteresis loops at quasistatic TDD oscillations

Indeed our limit hysteresis curves have two asymptotic components (see Fig. 5). The first one of them is connected with rolling and partially sliding rubber balls along spout guides without additional barriers.

Occurrence of the second asymptotic curve is concerned with strong deformation of balls due to support on the spout guides. It seems the first asymptote is the straight line. The second asymptote is not a straight line, but in the Fig. 5 it is represented as a straight line symbolically.

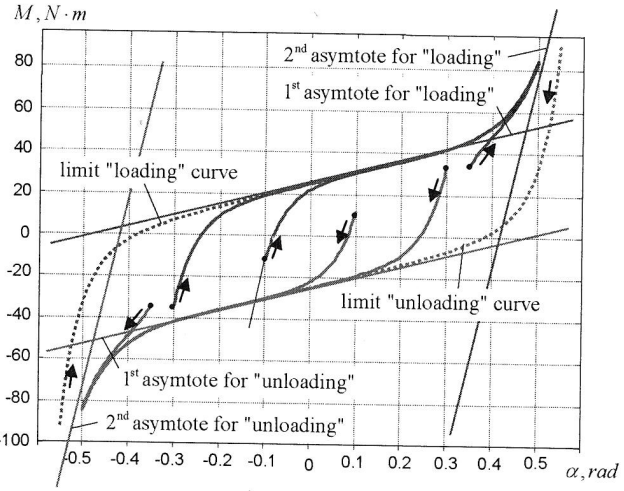

Fig. 5. Asymptotic tendency of internal curves to limit cycles curves

One of possible differential (kinematic) dependencies between torque and rotation angle can be taken as:

$$\frac{dM}{d\alpha} = \sum_{i=0}^{m} k_i \alpha^i + \sum_{i=0}^{n} c_i \alpha^i \cdot M \,, \quad . \tag{3}$$

where coefficients k_i $(i = 0,\ldots,m)$ and c_i $(i = 0,\ldots,n)$ are found via experimental limit cycle curve.

Therefore, first of all it needs to determine limit cycle curve experimentally. It is the dependence of torque versus relative angle of rotation: $M = M(\alpha)$.

The next step consists of approximating discrete data points by a spline. Mathematically, the problem is a trivial one because the limit cycle curve is a quite simple one. Analytical approximation of the limit cycle curve allows us to calculate derivatives $dM/d\alpha$ easily.

Let N is a total number of coefficients k_i $(i = 0,\ldots,m)$ and c_i $(i = 0,\ldots,n)$ in (4). This number determines a total number of algebraic equations for determination of these coefficients on the basis of (3). For that, we have to set N points on the limit curve and calculate derivatives at those points. It gives us a system of algebraic equations for determination of coefficients in (3).

After a series of numerical experiments, it was determined for (3) that $m = 1$, $n = 6$. Then, if to follow the technique described above, we obtain

$$k_0 = 650.9,\ k_1 = 1422.2;$$
$$c_0 = -23.9,\ c_1 = -4.1,\ c_2 = -2.0,\ c_3 = -0.35.5,\ c_4 = 143.2,\ c_5 = 419.8.$$

Then the equations (3) are written in a form

$$\frac{dM}{d\alpha} = k_0 + k_1\alpha + \left(c_0 + c_1\alpha + c_2\alpha^2 + c_3\alpha^3 + c_4\alpha^4 + c_5\alpha^5\right)M. \quad (4)$$

Note that equation (3) can be solved analytically. But it is not change the approach concept because of the right part of (3) can have another form with limit solution cycles.

3. Calculation of energy dissipated by the TDDs

There is of great interest to calculate capacity of dissipation (dissipation energy per unit of time) instead of full energy:

$$A = \frac{1}{t}\int_t M_1\, d\alpha = \frac{1}{t}\int_t M_1\dot{\alpha}\, dt. \quad (5)$$

Under the nonstationary motion, it is quite difficult to calculate the integral in (5). It is much simpler to convert (5) to a differential form and include the obtained equation to the system of equations (2), (4). By differentiation of (5) we have $t\dot{A} + A = M_1\dot{\alpha}$, from which we obtain differential equation

$$\frac{dA}{dt} = \frac{1}{t}\left(M_1\dot{\alpha} - A\right).$$

Solution of this equation has a horizontal asymptote, its ordinate giving the steady motion power of dissipation.

4. Some results of numerical analysis of TDD efficiency

Calculations were made for three TDD variants: an inertial and gravitational types (see Fig. 3), and a mixed type that have been produced at ESSP and tested further in Kazakhstan.

Configurations of inertial, gravitational and mixed types of TDD variants are presented in Fig. 6. The inertial and gravitational variants have one driving and one driven disks. The mixed variant has two external driven disks and one internal driving disk between driven disks. The rubber balls are inserted between driving and driven disks for all TDD variants.

Numerical scanning of parameters has been realized for all examined TDD variants. There were obtained the dissipation energy (dissipation capacity) values, transfer functions, as depending on driving frequency, and hysteresis dependence of torque versus relative rotation angle.

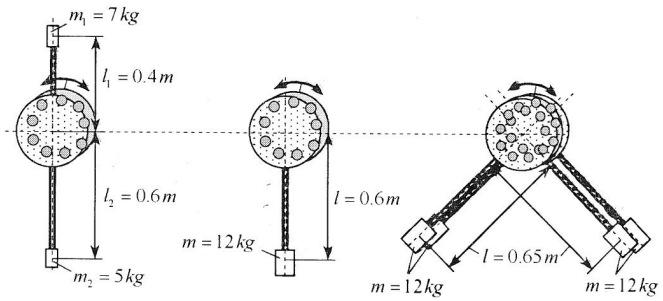

a) Inertia balancer b) Gravitational balancer c) Mixed type balancer

Fig. 6. Sketches of inertial, gravitational and mixed type TDD variants

As example, dissipation dependence (capacity) from driving frequency under input amplitude $\Phi = 0.3$ *rad* for the inertial (Fig. 6-a) and gravitational (Fig. 6-b) TDD variants is shown in Fig. 7.

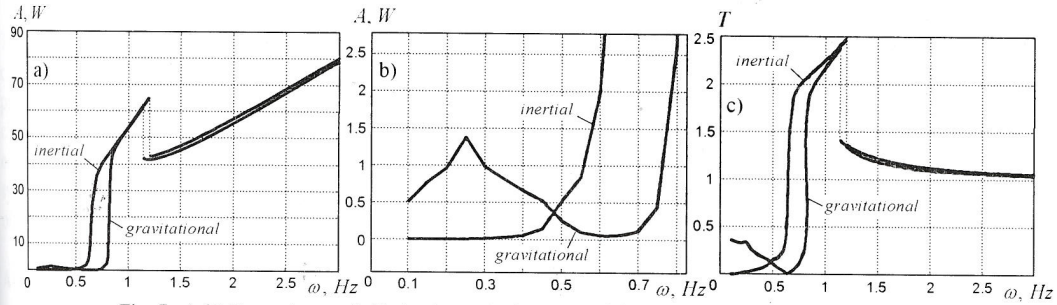

Fig. 7. a), b) Dependence of dissipation capacity versus driving frequency under input amplitude $\Phi = 0.3$ *rad* for the inertial and gravitational TDD versions; c) Transfer function

Hysteresis dependencies of torque (M) versus relative rotational angle (α) are presented in Figs. 8-11 at driving amplitude $\Phi = 0.3$ *rad* and frequencies $\omega = 0.2$, 0.4, 0.6 and 0.7 *rad*.

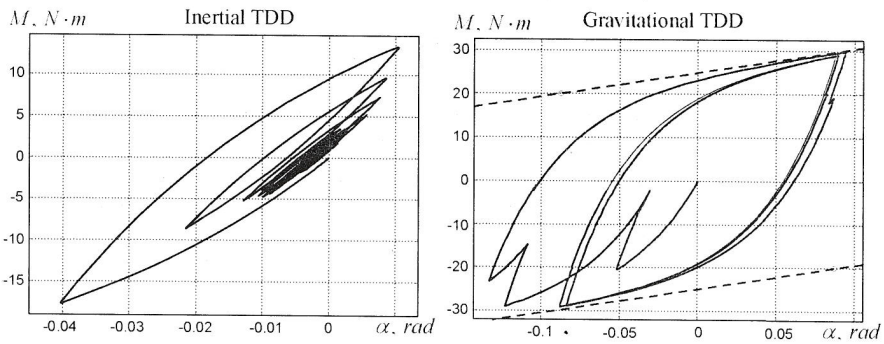

Fig. 8. Hysteresis dependences at $\Phi = 0.3$ *rad* and $\omega = 0.2$ *Hz*

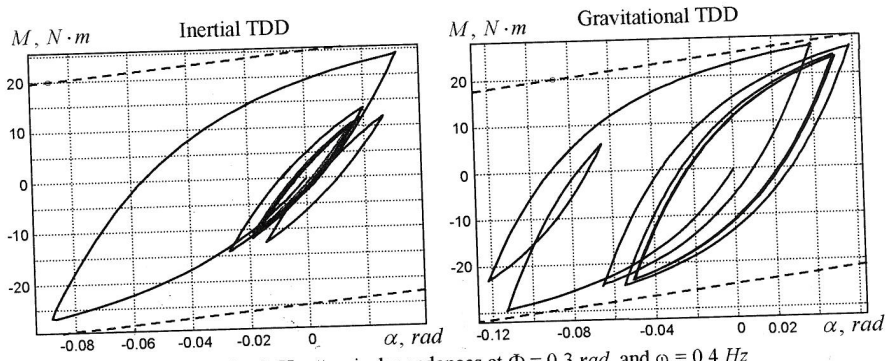

Fig. 9. Hysteresis dependences at $\Phi = 0.3$ *rad* and $\omega = 0.4$ *Hz*

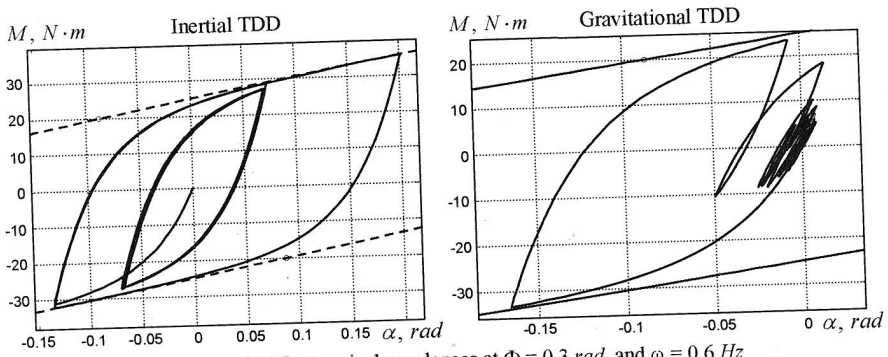

Fig. 10. Hysteresis dependences at $\Phi = 0.3$ *rad* and $\omega = 0.6$ *Hz*

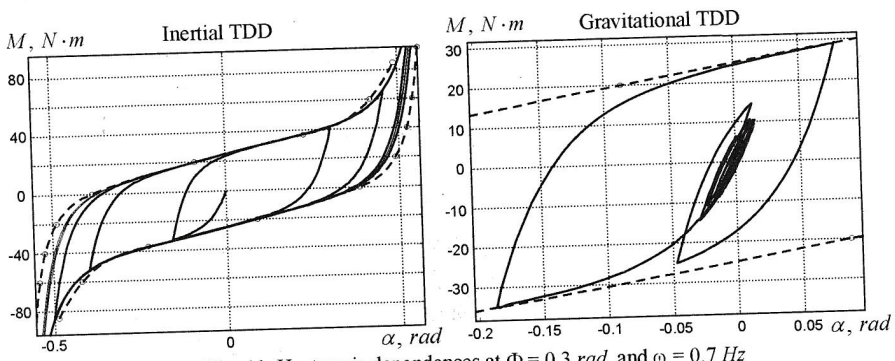

Fig. 11. Hysteresis dependences at $\Phi = 0.3$ *rad* and $\omega = 0.7$ *Hz*

In Fig. 12 results of calculations are given for the mixed type TDD variant (see Fig. 6-c) that has been produced at ESSP and tested further in Kazakhstan. The limit cycles curves were obtained experimentally on the stand at ESSP. These curves are shown by dotted lines in Fig. 13. Using these curves, the numerical experiment was carried out and it was compared with modeling of free TDD oscillations. Results are shown in Figs. 12, 13.

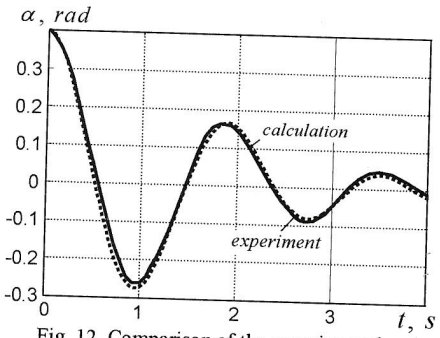

Fig. 12. Comparison of the experimental and theoretical results for the mixed type TDD version (see Fig. 6-c) in case of free oscillation decay (log. decr. value $\Delta = 1.4 \pm 0.05$ and natural freq. $\omega = 0.55\text{-}0.56$ *Hz* in both cases)

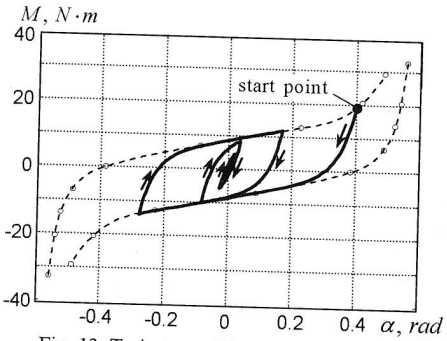

Fig. 13. Trajectory of hysteretic behavior of $M = M(\alpha)$ for the process displayed in Fig. 12

CONCLUSIONS

The approach proposed for the TDD efficiency analysis is based on differential dynamic equations compilation for all the structure units as a whole. Kinematic equation adequately describes basic principles of the damping unit action. This approach needs limited number of experiments to obtain characteristics required. The full system of the equations obtained can be composed with dynamic equations of OHL bundled conductors oscillations (with spacers installed) to obtain a generalized system of dynamics equations. Finally, there appears a possibility of searching optimal combinations of the TDD parameters on the basis of the approach proposed.

Acknowledgments

The work is fulfilled under support of INTAS Project 03-51-3736.

REFERENCES

[1] Damper for galloping conductors for overhead power transmission lines. Patent WO 2005/117228, PCT/RU2005/000302.

[2] A.A. Vinogradov, I.I. Sergey, N.M. Platonova, N.M. Rossukanyi, A.N. Danilin, V.I. Shalashilin, M.A. Djamanbaev, N.V. Shirinskih, F.N. Shklyarchuk and B. Konyrbayev. Progress report to the grant INTAS ID: 03-51-3736 "Control of Galloping on High Voltage Overhead Electrical Lines" over a period of time 01.09.2004-31.03.2006. Stage 2. Moscow. 2006.

[3] A.A. Vinogradov, I.I. Sergey, N.M. Platonova, N.M. Rossukanyi, A.N. Danilin, V.I. Shalashilin, M.A. Djamanbaev, N.V. Shirinskih, F.N. Shklyarchuk and B. Konyrbayev. Final report to the grant INTAS ID: 03-51-3736 "Control of Galloping on High Voltage Overhead Electrical Lines" over a period of time 01.04.2006-31.06.2007. Moscow. 2007.